Plant Physiology®

Plant Physiology, 2025, **197**, kiae551
https://doi.org/10.1093/plphys/kiae551
Advance access publication 17 October 2024
Research Article

Stomatal closure as a driver of minimum leaf conductance declines at high temperature and vapor pressure deficit in *Quercus*

Joseph Zailaa,[1,*] Christine Scoffoni,[2] Craig R. Brodersen[1]

[1]School of the Environment, Yale University, New Haven, CT 06511, USA
[2]Department of Biological Sciences, California State University, Los Angeles, Los Angeles, CA 90032, USA
*Author for correspondence: josephzailaa@gmail.com
The author responsible for distribution of materials integral to the findings presented in this article in accordance with the policy described in the Instructions for Authors (https://academic.oup.com/plphys/pages/General-Instructions) is: Joseph Zailaa.

Abstract

Rising global temperatures and vapor pressure deficits (VPDs) are increasing plant water demand and becoming major drivers of large-scale plant mortality. Controlling transient leaf water loss after stomatal closure (minimum stomatal conductance [g_{min}]) is recognized as a key trait determining how long plants survive during soil drought. Yet, substantial uncertainty remains regarding how g_{min} responds to elevated temperatures and VPD and the underlying mechanisms. We measured g_{min} in 24 *Quercus* species from temperate and Mediterranean climates to determine whether g_{min} was sensitive to a coupled temperature and VPD increase. We also explored mechanistic links to phenology, climate, evolutionary history, and leaf anatomy. We found that g_{min} in all species exhibited a nonlinear negative temperature and VPD dependence. At 25 °C (VPD = 2.2 kPa), g_{min} varied from 1.19 to 8.09 mmol m^{-2} s^{-1} across species but converged to 0.57 ± 0.06 mmol m^{-2} s^{-1} at 45 °C (VPD = 6.6 kPa). In a subset of species, the effect of temperature and VPD on g_{min} was reversible and linked to the degree of stomatal closure, which was greater at 45 °C than at 25 °C. Our results show that g_{min} is dependent on temperature and VPD, is highly conserved in *Quercus* species, and is linked to leaf anatomy and stomatal behavior.

Introduction

Rising global temperature and vapor pressure deficit (VPD) are increasing plant water use (Yuan et al. 2019; Grossiord et al. 2020; McDowell et al. 2022). Insufficient precipitation and desiccation ultimately lead to the hydraulic failure of plant vascular systems, thereby decoupling vegetation from the hydrological cycle (Choat et al. 2018). Large-scale forest tree mortality coupled with rising VPD is also linked to increased stand replacing fire probabilities (Brodribb et al. 2020; Nolan et al. 2020; Peters et al. 2021; Hammond et al. 2022; Ruffault et al. 2023). Plants typically close their stomata when moisture is limited to conserve water and prevent the buildup of excessive xylem sap tension leading to hydraulic failure (Martin-StPaul et al. 2017; Choat et al. 2018; Liang et al. 2023). Once stomata close, transient water loss to the atmosphere continues to occur across plant surfaces (Boyer et al. 1997; Schuster et al. 2017; Choat et al. 2018; Duursma et al. 2019). Water loss across the leaf epidermal cells, cuticle, and incompletely closed stomata, known as the leaf minimum conductance (g_{min}, unit: mmol m^{-2} s^{-1}), is recognized as a key trait that determines how long plants can survive during drought (Martin-StPaul et al. 2017; Hammond and Adams 2019; Brodribb et al. 2020), as g_{min} sets the rate at which water storage is lost to the surrounding atmosphere (Duursma et al. 2019).

g_{min} is typically measured under stable laboratory conditions at ~25 °C and low VPD (<2 kPa; Sack et al. 2011), where the leaf is conditioned to induce stomatal closure and is then repeatedly dried and weighed to measure the rate of water loss over time. However, leaf temperatures (T_L) vary over diurnal and seasonal timescales in the field. While standardized methodology allows for cross-study comparisons, it necessarily limits our ability to understand how g_{min} might vary under biologically relevant fluctuations in temperature and VPD. Indeed, little is known about how g_{min} responds to changes in air temperature and high VPD typical of drought-induced mortality events (Zhang et al. 2017). Understanding the temperature response of g_{min} during such conditions is therefore critical as vegetation models often assume a positive temperature dependence of g_{min}. For example, such models resulted in ~40% greater plant mortality globally than models assuming fixed g_{min} under projected climate scenarios (Brodribb et al. 2020; Cochard 2021). Yet, whether g_{min} is temperature dependent and whether the response amplitude is commonly shared across species within a habitat remain unclear, leading to uncertainty in how to appropriately model the response.

Conflicting evidence in the literature suggest positive or neutral temperature dependence for g_{min} in desert (Schuster et al. 2016; Bueno et al. 2019), temperate (Wang et al. 2024), and tropical species (Slot et al. 2021) and provide no clear explanations as to what is driving interspecific variability in g_{min}, primarily due to the limited number of species studied and lack of consistent methodology. These studies also fail to provide a mechanistic link between functional anatomy or physiology and observed temperature responses.

Anatomical traits that might influence g_{min} with changing temperature include, but are not limited to, cuticle thickness, cuticle chemistry, trichome density, stomatal size and density, and stomatal sensitivity to temperature, all of which could alter diffusion

Received July 25, 2024. Accepted October 1, 2024.

across the cuticle and leaf boundary layer (Cameron et al. 2006; Riederer and Muller 2006; Bi et al. 2017; Huggins et al. 2018; Machado et al. 2021; Grünhofer et al. 2022; Seufert et al. 2022; Ochoa et al. 2024). Further, cuticle waxes can melt at elevated temperatures between 60 and 80 °C (Eglinton and Hamilton 1967; Yeats and Rose 2013; Bueno et al. 2019), altering the rate of water diffusion across the cuticular surface. Cuticle permeability in response to temperatures elevated above 30 to 40 °C is unknown (Márquez et al. 2021). Finally, a major assumption of standardized lab-based g_{min} measurements is that stomata are fully closed and do not meaningfully contribute to cuticular and epidermal water loss (Sack et al. 2011), yet studies suggest that stomata may respond to temperature (Mansfield 1965; Pemdasa 1977; Hamerlynck and Knapp 1996; Mott and Peak 2010; Mathur et al. 2014; Marchin et al. 2022) and can be leaky after they are assumed to be closed, contributing to g_{min} (Kerstiens 1996; Duursma et al. 2019; Machado et al. 2021; Márquez et al. 2022; Ochoa et al. 2024). Further, nocturnal stomatal conductance has also been observed and can vary greatly across species (Mansfield 1965; Ehrler 1971; Pemdasa 1977; Benyon 1999; Musselman and Minnick 2000; Barbour et al. 2005; Bucci et al. 2005; Daley and Phillips 2006; Caird et al. 2007; Dawson et al. 2007; Marks and Lechowicz 2007; Novick et al. 2009; Mott and Peak 2010; Lombardozzi et al. 2015).

The purpose of this study was to investigate the temperature response of g_{min} and attempt to link any observed response to a mechanistic explanation. We constrained our taxa to a single genus (*Quercus*), as opposed to previous intergeneric studies (Slot et al. 2021), which has the benefit of determining some degree of congeneric variability. We selected 24 oak species (genus *Quercus* and subgenus *Quercus*) from four sections (*Quercus*, *Cerris*, *Lobatae*, and *Protoblanus*), divergent in climate of origin (Mediterranean or temperate), phenology (evergreen, deciduous, or brevideciduous), and anatomical and physiological traits that may influence observed g_{min} temperature responses. Oaks comprise a global clade, inhabiting various habitats, with important ecological and economical value (Cavender-Bares 2019; Hipp et al. 2020; Kremer and Hipp 2020). Oaks also present leaf morphological and anatomical differences even within the subgenus *Quercus* (Cavender-Bares 2019).

We developed 2 working hypotheses that guided our investigation into the temperature response of g_{min}: (i) if g_{min} is determined solely by cuticle permeability properties and/or stomatal aperture is not influenced by temperature/VPD, then increasing temperatures increase VPD and therefore increase the driving force for the evaporation of water across the cuticle and partially open stomata, leading to a positive temperature response and (ii) if stomatal aperture in leaky stomata is influenced by ambient temperature (Hamerlynck and Knapp 1996; Marchin et al. 2022) and stomata could close more completely at higher temperatures or cuticular waxes can melt and rearrange or expand at elevated temperatures, then leaves would present a negative relationship between g_{min} and temperature. We expected that if any observed short-term temperature response of g_{min} is due to physical changes in cuticular structure (e.g. melting, rearranging, and expansion of cuticular waxes; Schreiber 2001), then the observed response may be irreversible; while if g_{min} response is due to stomatal sensitivity to temperature, then the observed response may be reversible between high and low temperatures.

Because of their evolutionary history and long-term adaptation to arid habitats (Kremer and Hipp 2020), we expected that evergreen species and those from Mediterranean climates (MC) should show a weaker temperature response if g_{min} is positively related to temperature or a stronger response if g_{min} is negatively related to temperature, than deciduous and brevideciduous species or those from more mesic, temperate climates (TC). Such a response would prevent excessive water loss in species regularly exposed to drought conditions or species that have to maintain their leaves through seasonal fluctuations in temperature. We also expected g_{min} could be correlated with other leaf traits such as (i) cuticular texture and the presence or absence of hairs because these would alter the epidermal and cuticular surface area from which water could diffuse, (ii) stomatal density (SD, mm^{-2}) since a greater SD increases the porosity of the leaf provided imperfectly closed stomata, or (iii) with traits such as leaf area (LA, mm^2) and leaf mass per area (LMA, $g\ m^{-2}$) as previously found in other studies (Wang et al. 2019; Slot et al. 2021).

Results

Negative temperature and VPD response of g_{min}

We found that g_{min} declined with increasing temperature and VPD in all 24 *Quercus* species (Supplementary Fig. S1 and Tables S1 and S2; Table 1). The mean g_{min} across all species declined from 2.83 ± 0.31 to 1.34 ± 0.13 and 0.57 ± 0.05 mmol m^{-2} s^{-1} at 25, 35, and 45 °C, respectively (Table 1). We found the greatest variability in g_{min} at 25 °C, from 1.19 to 8.09 mmol m^{-2} s^{-1} in *Quercus coccinea* and *Q. durata*, respectively (Table 1). This range constitutes 0.4% to 2.5% of g_{max} values reported in the literature for 10 of our study species for which g_{max} data were available in the literature (Jurik 1986; Reich and Hinckley 1989; Loewenstein and Pallardy 1998; Matsumoto et al. 1999; Wilson et al. 2000; Xu and Baldocchi 2003; Schäfer 2011; Dillen et al. 2012; Meinzer et al. 2017; Henry et al. 2019). Both intraspecific and interspecific variabilities in g_{min} were low at the 35 and 45 °C temperature conditions (Table 1; Supplementary Fig. S1). Further, the slope of g_{min} as a function of temperature varied considerably across species, 8.2-fold, 7.4-fold, and 7.2-fold and averaged -0.15 ± 0.02, -0.08 ± 0.01, and -0.11 ± 0.01 mmol m^{-2} s^{-1} $°C^{-1}$, from 25 to 35, 35 to 45, and 25 to 45 °C, respectively (Table 1). Our calculations of the relative water content (RWC) of the leaves we measured show that the mean RWC of our leaves was $77.7 \pm 1.2\%$ SE across all measurements and temperature steps with a mean max intraspecific difference of $8.6 \pm 1.0\%$ SE between temperature steps across all species (Supplementary Table S3).

Climatic, phenological, evolutionary, and anatomical correlations with g_{min}

We found climatic, evolutionary, and anatomical-correlated relationships between g_{min} and its response to temperature, but no phenologically correlated differences in g_{min}-related traits (ANOVA $P > 0.05$ for all traits; Fig. 1). Species with a rough cuticular surface texture had higher g_{min} at all 3 temperatures and a more negative slope of g_{min} as a function of temperature from 25 to 35 °C and from 25 to 45 °C (ANOVA $P = 0.002$ to 0.038), but not between 35 and 45 °C (ANOVA $P > 0.05$) compared with species with a smooth cuticular texture (Fig. 1A). The g_{min} temperature responses also differed between taxa of TC and MC species. MC species had a greater g_{min} at all 3 temperatures and a more negative slope of g_{min} as a function of temperature from 35 to 45 °C (ANOVA $P = 0.003$ to 0.027), but not between 25 and 35 °C or 25 and 45 °C (ANOVA $P > 0.05$; Fig. 1D). Finally, we found evolutionary correlations between g_{min} and species from different *Quercus* sections. Species from section *Quercus* had a greater g_{min} than species from section *Lobatae*, while species from section *Cerris* had similar g_{min} to species from sections *Quercus* and *Lobatae* at all 3 temperatures (ANOVA $P = 0.005$ to 0.017) and sections did not differ in

Table 1. Phylogenetic, phenological (deciduous, D; evergreen, E; and brevidecidous, B), climate (temperate climate, TC vs. MC), and leaf cuticular descriptive (rough vs. smooth cuticle; presence, P; or absence A, of trichomes) data for all *Quercus* taxa used in the study, in addition to mean g_{min} data at the 3 sampled temperatures and leaf trait data

Species	Section	Phenology	Climate	Cuticular surface	Trichome (P/A)	g_{min}			SD	LMA	LA	LT
						At 25 °C mmol m^{-2} s^{-1}	At 35 °C mmol m^{-2} s^{-1}	At 45 °C mmol m^{-2} s^{-1}	mm^{-2}	g m^{-2}	cm^2	mm
Q. acutissima	*Cerris*	D	TC	Smooth	A	2.04 ± 0.09	0.86 ± 0.04	0.41 ± 0.02	781 ± 175	85 ± 7	39.8 ± 5	0.14 ± 0.01
Q. agrifolia	*Lobatae*	E	MC	Smooth	P	1.66 ± 0.34	1.01 ± 0.28	0.34 ± 0.07	307 ± 44	142 ± 4	6.9 ± 2	0.22 ± 0
Q. alba	*Quercus*	D	TC	Rough	P	1.92 ± 0.25	0.86 ± 0.14	0.39 ± 0.03	663	85 ± 5	65.1 ± 5.4	0.14 ± 0.02
Q. berberidifolia	*Quercus*	B	MC	Rough	P	3.59 ± 0.6	1.65 ± 0.09	0.67 ± 0.09	472 ± 113	172 ± 4	2.8 ± 0.1	0.28 ± 0.01
Q. bicolor	*Quercus*	D	TC	Smooth	P	3.15 ± 0.28	1.69 ± 0.11	0.62 ± 0.04		87 ± 8	58.5 ± 1.7	0.14 ± 0.01
Q. chrysolepis	*Protobalanus*	E	MC	Rough	P	1.38 ± 0.16	0.77 ± 0.15	0.37 ± 0.09	557 ± 59	192 ± 20	4.7 ± 1.3	0.34 ± 0.04
Q. coccinea	*Lobatae*	D	TC	Smooth	A	1.19 ± 0.05	0.48 ± 0.05	0.2 ± 0.02	684 ± 34	76 ± 5	63.7 ± 6.5	0.13 ± 0.01
Q. douglasii	*Quercus*	D	MC	Rough	P	5.53 ± 0.64	2.84 ± 0.26	1.2 ± 0.17	382	147 ± 11	6.3 ± 1.2	0.26 ± 0.02
Q. durata var. *durata*	*Quercus*	E	MC	Rough	P	8.09 ± 1.03	3.09 ± 0.86	1.06 ± 0.16	506	197 ± 12	2.9 ± 0.7	0.26 ± 0.01
Q. engelmannii	*Quercus*	B	MC	Rough	P	3.69 ± 0.59	1.77 ± 0.23	0.92 ± 0.17	569	173 ± 12	6.4 ± 0.4	0.33 ± 0.02
Q. garryana var. *garryana*	*Quercus*	D	MC	Rough	P	3.54 ± 0.41	1.73 ± 0.12	0.95 ± 0.14		134 ± 2	25.6 ± 4.3	0.21 ± 0.01
Q. john-tuckeri	*Quercus*	E	MC	Rough	P	2.44 ± 0.32	1.06 ± 0.02	0.58 ± 0.1		219 ± 12	1.8 ± 0.1	0.34 ± 0.02
Q. kelloggii	*Lobatae*	D	MC	Smooth	P	2.14 ± 0.33	1.01 ± 0.1	0.43 ± 0.11	375	115 ± 8	22.3 ± 3.8	0.16 ± 0.01
Q. lobata	*Quercus*	D	MC	Rough	P	3.53 ± 0.38	1.84 ± 0.18	0.84 ± 0.01	395	115 ± 8	19.4 ± 2.3	0.2 ± 0
Q. macrocarpa	*Quercus*	D	TC	Rough	P	3.61 ± 0.51	1.54 ± 0.23	0.68 ± 0.1		79 ± 8	97.8 ± 22.1	0.16 ± 0.03
Q. montana	*Quercus*	D	TC	Rough	P	2.59 ± 0.58	1.26 ± 0.15	0.51 ± 0.14	520	71 ± 7	96.8 ± 7.2	0.14 ± 0.01
Q. muehlenbergii	*Quercus*	D	TC	Rough	P	1.79 ± 0.17	0.81 ± 0.13	0.34 ± 0.03		64 ± 3	53.7 ± 5.9	0.11 ± 0
Q. pacifica	*Quercus*	B	MC	Rough	P	3.43 ± 0.46	1.87 ± 0.26	0.74 ± 0.05	316 ± 16	138 ± 20	4.1 ± 0.9	0.23 ± 0.03
Q. palustris	*Lobatae*	D	TC	Smooth	A	1.84 ± 0.19	0.62 ± 0.08	0.25 ± 0.03	417 ± 30	67 ± 3	41 ± 8	0.12 ± 0
Q. prinus	*Quercus*	D	TC	Rough	P	2.7 ± 0.09	1.39 ± 0.06	0.53 ± 0.01	595	93 ± 11	54.6 ± 3	0.17 ± 0.02
Q. rubra	*Lobatae*	D	TC	Smooth	P	1.2 ± 0.02	0.57 ± 0	0.22 ± 0.01	383 ± 27	83 ± 7	91.3 ± 22.9	0.14 ± 0.01
Q. variabilis	*Cerris*	D	TC	Smooth	P	1.92 ± 0.23	1 ± 0.1	0.4 ± 0.05		73 ± 3	45.8 ± 4	0.13 ± 0.01
Q. velutina	*Lobatae*	D	TC	Smooth	P	2.13 ± 0.37	1.01 ± 0.24	0.45 ± 0.13	494 ± 166	78 ± 2	65.4 ± 10.3	0.15 ± 0.02
Q. wislizeni	*Lobatae*	E	MC	Smooth	A	2.75 ± 0.44	1.55 ± 0.16	0.56 ± 0.03	357	164 ± 4	4.4 ± 0.7	0.28 ± 0.01

Leaf trait data include SD, LMA, LA, and LT. Reported values are means ± 1 SE for all 24 species. When means are absent, we could not measure a trait for certain species, and when SE values are absent, less than 3 individuals were measured for that species.

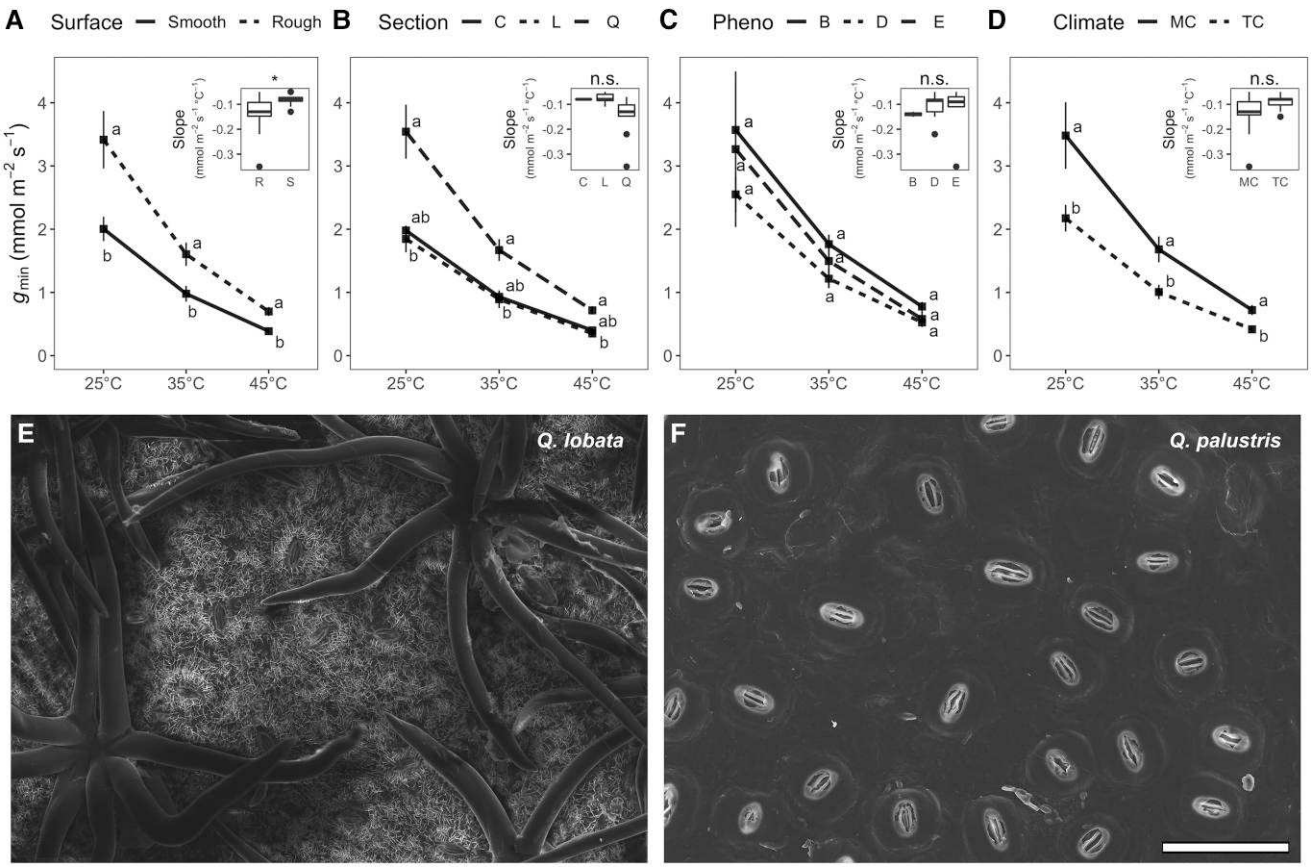

Figure 1. The response of g_{min} to increasing ambient temperature of 24 *Quercus* species. Species are grouped by **A)** cuticular appearance: rough ($n = 14$ species) vs smooth cuticles ($n = 10$ species), **B)** phylogenetic placement: *Quercus* ($n = 14$ species) vs *Lobatae* ($n = 7$ species) vs *Cerris* ($n = 2$ species), **C)** phenology: evergreen ($n = 5$ species) vs deciduous ($n = 16$ species) vs brevideciduous ($n = 3$ species), **D)** climate of origin: temperate climate ($n = 12$ species) vs Mediterranean climate ($n = 12$ species). **E** and **F)** Scanning electron micrographs of representative species with a rough vs smooth texture of the abaxial cuticular surface. Scale bar is 50 μm for both images. Error bars represent 1 SEM. Lowercase letters represent Tukey post hoc test and apply to all statistical analysis results as shown in the main plot **A** to **D)**. Additionally, the insets show the differences in slopes between 25 and 45 °C (unit: mmol m^{-2} s^{-1} °C^{-1}) and results of a 1-way ANOVA between groups. n.s., not significant; *$P < 0.05$. Center line, median; box limits, upper and lower quartiles; whiskers, 1.5× interquartile range; points, outliers.

the slope of g_{min} as a function of temperature from 25 to 35 °C, 35 to 45 °C, or 25 to 45 °C (ANOVA $P > 0.05$; Fig. 1B).

Relationships between leaf traits and g_{min} traits

We found that g_{min} at all 3 temperatures correlated positively with LMA ($r = 0.46$ to 0.56; $P = 0.005$ to 0.025; Supplementary Table S4) and negatively with LA ($r = -0.48$ to -0.43; $P = 0.019$ to 0.037; Supplementary Table S4). Leaf thickness (LT) also correlated positively with g_{min} at 45 and 35 °C but not at 25 °C ($r = 0.47$ to 0.53; $P = 0.008$ to 0.022; Supplementary Table S4). Further, LMA correlated negatively with the slope of g_{min} as a function of temperature from 25 to 35 °C, 35 to 45 °C, and 25 to 45 °C ($r = -0.46$ to -0.41; $P = 0.025$ to 0.042; Supplementary Table S4), with species with higher LMA exhibiting steeper declines. LMA also correlated negatively with LA ($r = -0.94$; $P < 0.001$; Supplementary Table S4) and positively with LT ($r = 0.96$; $P < 0.001$; Supplementary Table S4). TC species had a significantly higher LA and lower LMA and LT than MC species (ANOVA $P < 0.001$). We found no correlation between stomatal and trichome density with g_{min} ($P > 0.05$; Supplementary Table S4).

Reversible changes in g_{min} temperature response

For a subset of species ($n = 4$), we found that g_{min} declined when temperature increased from 25 to 45 °C and that when leaves transition from 45 °C back to 25 °C, g_{min} returned to the original steady-state value (Fig. 2; Supplementary Table S2). Thus, the temperature response was reversible in at least 4 *Quercus* species (*Q. coccinea*, *Q. douglasii*, *Q. durata*, and *Q. rubra*; Fig. 2; Supplementary Table S2). Leaves from all species that were initially acclimated to 45 °C that were then cooled to 25 °C experienced an increase in g_{min}, while leaves that were initially acclimated to 25 °C and then heated to 45 °C experienced a decrease in g_{min} (Fig. 2; Supplementary Table S2).

Contribution of stomatal pore area to g_{min} temperature response

In situ micro-CT image analysis revealed that both *Q. douglasii* and *Q. durata* had partially open stomata despite being semidehydrated, in the dark, and under conditions that are typically thought to induce full stomatal closure (Fig. 3; Supplementary Table S5). Paradermal and transverse micro-CT images (Fig. 3) clearly show both open and partially closed stomata when exposed to conditions similar to those used for lab-based g_{min} measurements. The magnification and resolution of the micro-CT images allowed us to measure the total number of stomata in the field of view, the percentage of those stomata that were open, partially closed, or fully closed, as well as their apertures (Fig. 3; Supplementary Table S5). Both species had ~55% of their

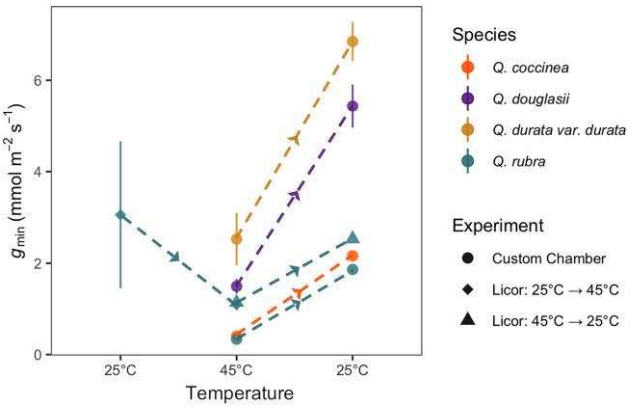

Figure 2. g_{min} as a function of temperature and the reversibility of the effect in 4 *Quercus* species. All species studied show a decline in g_{min} transitioning from 25 to 45 °C (Table 1; Supplementary Fig. S1), and a subset of 4 species return to original values at 25 °C. Circles represent data from the experiment where the same leaves from each individual per species were measured using the custom environmental chamber at 45 °C for 3 h and then at 25 °C for 2 h ($n = 3$ individuals per species). Diamonds represent data from the experiment where the same leaf was measured in the LI-6800 at 25 °C and warmed to 45 °C after steady state ($n = 3$ individuals per species). Triangles represent data from the experiment where the same leaf was measured in the LI-6800 at 45 °C and cooled to 25 °C after steady state ($n = 1$ individual per species). Each experiment was conducted on a different set of leaves. Error bars represent 1 SEM.

stomata open (ANOVA $P > 0.05$; Fig. 4A; Supplementary Table S4), but that percentage did not change with increasing ambient temperature (ANOVA $P > 0.05$; Fig. 4A; Supplementary Table S5). The mean pore area declined by over 48% and 49% in *Q. douglasii* and *Q. durata*, respectively, from 25 to 45 °C (ANOVA $P < 0.001$; Fig. 4B; Supplementary Table S5). At 45 °C, more stomata were fully closed in both species, and the distribution of stomatal pore area became more skewed toward smaller apertures (Fig. 4C; Supplementary Table S5). The distributions of stomatal pore area were significantly different in *Q. douglasii* and *Q. durata* at 25 and 45 °C (Kolmogorov–Smirnov test (KS) $P < 0.001$ and $P = 0.001$, respectively; Fig. 4C; Supplementary Table S5) and between *Q. douglasii* and *Q. durata* at 25 °C (KS $P = 0.035$; Fig. 4C; Supplementary Table S5) but not at 45 °C (KS $P > 0.05$; Fig. 4C; Supplementary Table S5).

Finally, modeling diffusion through partially open stomata using the Franks and Beerling (2009) equations suggests changes in stomatal pore area from 25 to 45 °C result in a 40.9 ± 4.6% and 45.1 ± 0.5% decrease in conductance in *Q. douglasii* and *Q. durata*, respectively, while measured g_{min} values show a 78.4 ± 1.7% and 86.9 ± 1.4% decrease in g_{min} from 25 to 45 °C in *Q. douglasii* and *Q. durata*, respectively (Supplementary Table S6).

Negative g_{min} temperature response delays plant senescence under simulated drought

We then used the SurEau model populated with our negative g_{min} temperature response to determine the effect on physiology and mortality in a simulated drought. Simulations where leaves had a positive temperature dependence for g_{min} resulted in plant mortality of 12.3 ± 3 d earlier compared with those assuming no temperature dependence under a MC scenario (Fig. 5). When we modeled mortality using the negative temperature dependence measured in this study, we found that leaves survived an additional 2.6 ± 0.6 d longer (Fig. 5). This was due to a delay in reaching lethal leaf water potential thresholds, which is directly related to this water saving function of more tightly closed stomata in response to elevated temperature. Simulations under the TC scenario did not result in plant mortality regardless of whether g_{min} was negatively, positively, or not dependent on temperature.

Discussion

Our data provide a comparison of g_{min} temperature and VPD responses for 24 *Quercus* representatives, with species divergent in habitat, life history traits, leaf anatomy, and morphology. We found that g_{min} consistently declined with increasing temperature and VPD. The consistent pattern leads us to conclude that this trait may be highly conserved within the genus but with significant variability in the magnitude of the effect. Given that there are 469 accepted species within this genus (POWO 2024), we are limited in our ability to extrapolate beyond our sampling, but our study taxa include mesic, xeric, deciduous, evergreen, and brevideciduous representatives from 4 different sections within the *Quercus* subgenus.

Our results support some of our hypotheses regarding the drivers of g_{min} and its temperature and VPD response in *Quercus*. Species with a rough cuticular texture exhibited a higher overall g_{min} across all 3 temperatures, suggesting a possible mechanistic link to cuticular anatomy (Fig. 1A). Higher g_{min} in rough cuticle species may be due to the increased surface area for diffusion of water across the leaf surface compared with smooth, unbroken cuticular surfaces, and/or a more porous medium of the waxy rod-like matrix of epicuticular waxes in rough cuticle species (Koch and Barthlott 2006; Sharma et al. 2018; Seufert et al. 2022). Divergent chemical compositions of epicuticular waxes may also influence the response (Bueno et al. 2019). While we did not measure the chemical composition of the cuticles, our results suggest that the magnitude of g_{min} and its response to temperature can be partially attributed to cuticular anatomy and possibly the epicuticular wax composition.

We also found differences in g_{min} between species belonging to different sections of the *Quercus* subgenus, suggesting an evolutionarily driven divergence in the magnitude of the g_{min} temperature response. We did not, however, find any phenologically correlated differences in g_{min}, suggesting that phenology and g_{min}-related traits may have evolved independently during the divergence of subgenus *Quercus* sections or possibly because we only sampled the youngest fully expanded leaves of the evergreen species we measured. Older stomata in evergreen species may become incontinent and can contribute to increased g_{min} in leaves retained for multiple growing seasons (Jordan and Brodribb 2007). Future studies can investigate how g_{min} is affected by leaf age in evergreen *Quercus* species.

Finally, contrary to our hypothesis, we found that MC species had a higher g_{min} than TC species, but a steeper response to increased temperature and VPD, especially between 25 and 35 °C. g_{min} has been reported as either higher or the same in species adapted to mesic environments compared with those from xeric environments (Smith et al. 2006; Burghardt et al. 2008; Saito and Futakuchi 2010; Brodribb et al. 2014; Hartill et al. 2023). Both g_{min} and stomatal conductance can increase during heat waves or high irradiance, which offers some evaporative cooling to lower T_L (Burghardt et al. 2008; Marchin et al. 2022). Similarly, as MC species experience higher seasonal air temperatures than temperate species, a higher g_{min} would be beneficial for T_L regulation. Further, we found that most MC species and those from the section *Quercus* exhibited a rough cuticular texture, while most TC

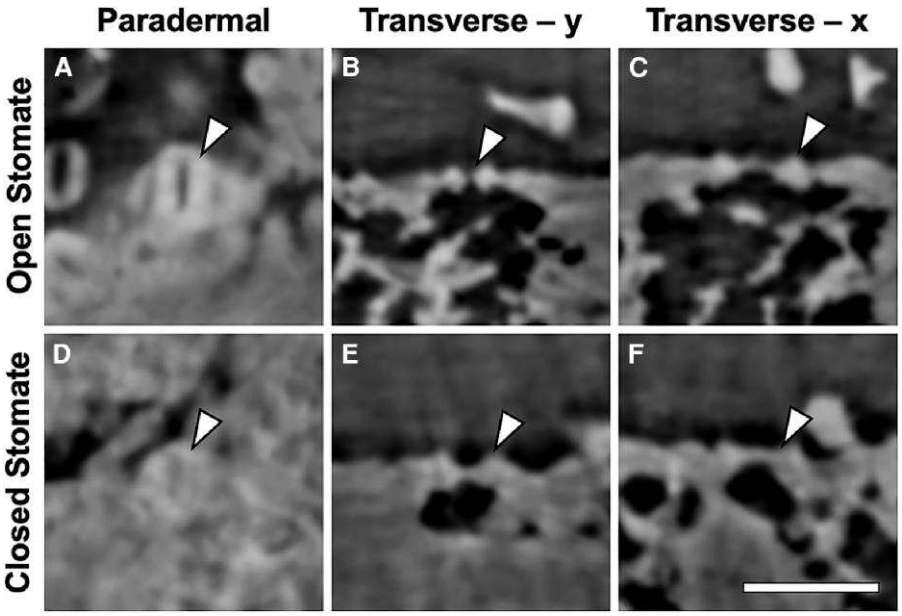

Figure 3. Representative paradermal and transverse in situ X-ray micro-CT images of open and closed stomata in *Q. douglasii*. A major advantage of micro-CT compared with other imaging or microscopy techniques is that the imaging plane can be perfectly aligned in either the paradermal **A** and **D)** or transverse plane **B**, **C**, **E**, and **F)** to be orthogonal to the desired plane of interest that reveals the stomatal pore. Open stomata and the pore aperture can be observed **A**, **B**, and **C)**, where the pore area and substomatal cavity are filled with air (black pixels) and the cells are hydrated (light gray and white pixels). Closed stomata are clearly visible and show no stomatal pore area, with the guard cells pressed together. **B**, **C**, **E**, and **F)** Show the orthogonal planes through the same stomata in **A** and **D)**. Arrows point to the same guard cell in panels **A** to **C)** and **D** to **F)**. Scale bar is 0.1 mm for all panels.

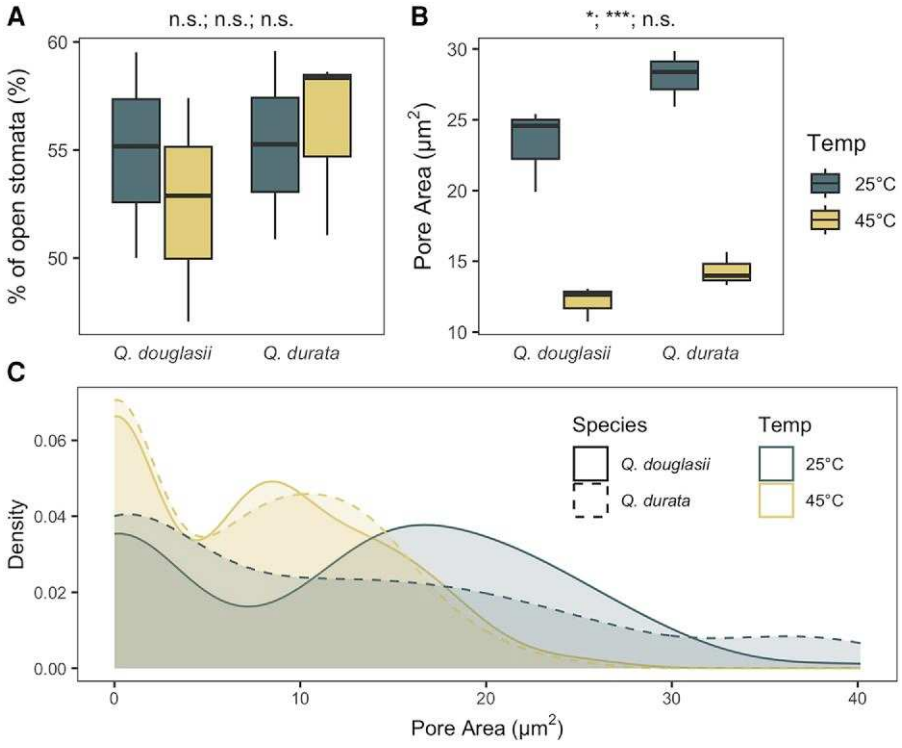

Figure 4. In situ X-ray micro-CT image analysis of the functional status of 99 stomata measured from 3 leaves per species for *Q. douglasii* and *Q. durata*. **A)** The percentage of open stomata for both species at 25 and 45 °C in intact leaves exposed to identical conditions as used for lab-based g_{min} measurements. **B)** Stomatal pore area calculated from measured apertures in the micro-CT images at the 2 temperatures. **C)** Stomatal pore area distributions for *Q. durata* and *Q. douglasii* measured from 99 stomata from each of 3 individuals per species. Asterisks denote 2-way ANOVA results for species, temperature, and species × temperature, respectively, and apply to all statistical analysis results as shown in the figure. n.s., not significant; $^{*}P < 0.05$; $^{***}P < 0.001$. Center line, median; box limits, upper and lower quartiles; whiskers, 1.5× interquartile range; points, outliers.

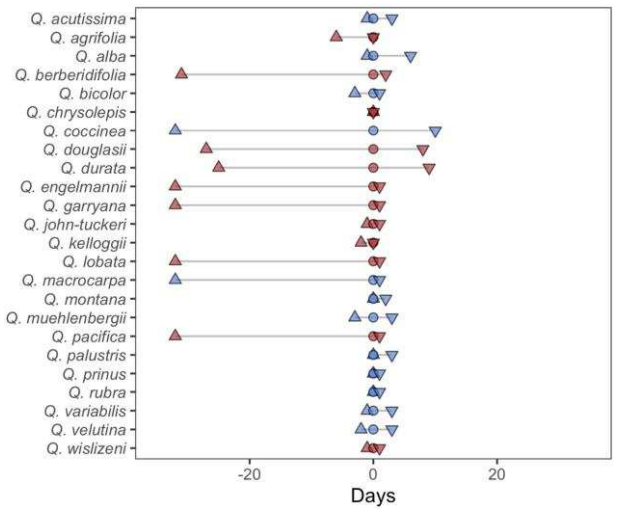

Figure 5. Modeled survival indices from the SurEau-Ecos simulation using g_{min} temperature response data from the present study. Results suggest differences in survival in days for the 24 *Quercus* species with a positive temperature response of g_{min} (triangles) and negative temperature response of g_{min} (inverted triangles) relative to no g_{min} temperature dependence (circles) under a simulated Mediterranean climate drought. Red and blue highlights denote species sampled from the California Botanical Garden and the Arnold Arboretum, respectively.

species and those from the other 3 sections of subgenus *Quercus* had a smooth cuticular texture, which could explain the similarities in g_{min} values between those groups (Fig. 1A, B, and D).

g_{min} correlated with some hypothesized leaf traits. g_{min} had a positive correlation with LMA but negative with LA across all 3 temperatures, contrary to what was found for 24 diverse tropical species (Slot et al. 2021), but similar to 16 temperate tree species (Wang et al. 2019). LT also correlated positively with g_{min} at 35 and 45 °C but not at 25 °C, which partially supports the findings of another study showing a positive correlation between LT and g_{min} in tomatoes under well-watered conditions (Dariva et al. 2020), though it is possible that the error of the calipers may have influenced these results. Further, we found no relationship between stomatal and trichome density with g_{min}, which also contradicts findings from other studies where higher g_{min} was associated with higher SD (Muchow and Sinclair 1989) or greater SD and length (Saito and Futakuchi 2010). Thus, our data further support the idea that g_{min} is highly variable across taxa, both in absolute values and in the magnitude of the response to elevated temperatures and VPD, and many leaf traits likely contribute to g_{min}.

Our data show that the temperature response of g_{min} was reversible, with a putative link to the degree of stomatal closure at each temperature step. In 4 taxa, g_{min} reverted to original values after heating or cooling to 45 or 25 °C, suggesting that changes in g_{min} are not driven by permanent changes such as cuticular waxes melting and becoming less permeable. It is possible that the cuticle's ability to self-assemble during formation (Koch and Barthlott 2006; Koch and Ensikat 2008) provides it with resilience against deforming within the temperature range measured in this study, which may have not exceeded the transition-phase temperature observed in other studies (Schreiber 2001; Bueno et al. 2019). Instead, we suggest that a considerable amount of the g_{min} temperature response in our study is due to reversible stomatal closure, particularly in species which showed a strong g_{min} response to temperature and VPD relative to others (Figs. 3 and 4). The g_{min} temperature response is possibly a result of increased leaf abscisic acid production in response to changes in VPD (Cardoso et al. 2020; Binstock et al. 2024) or more passive hydraulic mechanisms (Merilo et al. 2018). Future studies could investigate the mechanism behind the stomatal responses to VPD in dehydrated leaves.

Our most significant finding is related to the degree of stomatal closure in response to increasing temperature during g_{min} measurements. Up to 57% of stomata on leaves of 2 species were at least partially open despite being partially dehydrated and placed in the dark to induce complete stomatal closure. Indeed, studies have shown that nocturnal stomatal conductance can be a significant phenomenon (Mansfield 1965; Ehrler 1971; Pemdasa 1977; Benyon 1999; Musselman and Minnick 2000; Barbour et al. 2005; Bucci et al. 2005; Daley and Phillips 2006; Caird et al. 2007; Dawson et al. 2007; Marks and Lechowicz 2007; Novick et al. 2009; Mott and Peak 2010; Lombardozzi et al. 2015). Additionally, a study suggests that water loss through the epidermis *Q. rubra* shifts from being dominated by cuticular conductance during leaf expansion to loss from stomata at leaf maturity, further supporting our findings that stomata contribute to g_{min} in oak species (Kane et al. 2020). Furthermore, the temperature sensitivity of stomata exposed to elevated temperatures is directly observable with micro-CT imaging, which allowed us to not only determine the number of partially open stomata but also their aperture. A growing body of work has shown that stomata respond to changes in temperature (Mansfield 1965; Pemdasa 1977; Hamerlynck and Knapp 1996; Mott and Peak 2010; Mathur et al. 2014; Marchin et al. 2022), but these studies rarely control for the coordinated changes in VPD with temperature (Mills et al. 2024). Future work should investigate how both stomatal and cuticular conductances respond to temperature, independent of VPD.

Our data provide direct, visual evidence supporting this idea that stomata respond to changes in temperature and provide a means of measuring stomatal aperture in situ. Our micro-CT imaging method required that the leaves were completely enclosed in Kapton tape to prevent tissue dehydration during the scanning period. This treatment therefore greatly reduced the volume of air surrounding the leaf, likely leading to a high local relative humidity (RH) adjacent to the leaf surface, reducing VPD. Therefore, this experiment provides information about stomatal closure in response to temperature alone since VPD remained effectively constant. Thus, it is possible that an even greater reduction in stomatal aperture may occur with the combined effects of elevated temperature and VPD. This finding is significant in that it necessitates a consideration that much of the changes in g_{min} with elevated temperature can be attributed to partial stomatal closure and changes in stomatal aperture with temperature as opposed to changes in other traits that might determine the flux of water across the cuticle. Studies have shown that leaky stomata can contribute to residual water loss from the leaf (Burghardt and Riederer 2003; Šantrůček et al. 2004; Machado et al. 2021), but no study has yet quantified changes in this contribution with temperature associate to increased VPD. It is therefore difficult to fully understand the temperature dependence of g_{min} previously reported without knowing the degree of stomatal opening and stomatal temperature responses. There is likely variability across our study species, and we only imaged the 2 species with the steepest response of g_{min} to temperature. It is possible that stomata in species with milder responses of g_{min} to temperature were already shut tightly at 25 °C and could not shut tighter in response to temperature.

Our vapor diffusion modeling was able to assign only ~52% of the change in g_{min} to stomatal closure, however (Supplementary

Table S6). This may be due to variability between leaves or in stomatal closure across the leaf surface outside the field of view of our observations and a relatively small sample size for the micro-CT measurements and suggests a possible response of cuticular water conductance to temperature and VPD. Both taxa used for the micro-CT imaging had a rough cuticular surface, and thus we could not compare our results with species with smooth cuticles. Because of the high degree of technical difficulty in performing the micro-CT measurements and limited access to the micro-CT facility, we were unable to extend the findings to other taxa in our study, but this could be the focus of future work. Future studies could also investigate how differences in cuticular properties could affect the response of cuticular conductance and g_{min} to temperature and VPD.

Our results contrast with other studies investigating the g_{min} temperature response (Burghardt et al. 2008; Schuster et al. 2016; Bueno et al. 2019; Slot et al. 2021; Hartill et al. 2023), which report either positive or neutral temperature responses. Our results show that g_{min} can be negatively related to temperature and VPD and that this relationship may be conserved across the *Quercus* genus, although a positive temperature response has been shown recently for one *Quercus* hybrid species (Wang et al. 2024). Indeed, phenotypic plasticity has been observed for hydraulic traits including stomatal behavior and leaf gas exchange (Saruwatari and Davis 1989; Scoffoni et al. 2015; Herrera et al. 2022), as well as for cuticular anatomy and composition and their effect on cuticular conductance (Hlwatika and Bhat 2002; Zhang et al. 2021). It is also possible that discrepancies in these studies may be due to varying levels of leaf dehydration or RWC of leaves at the time of measurement (Boyer 2015), yet more work is needed to fully understand how leaf hydration levels affect g_{min}.

Finally, our simulations using the SurEau-Ecos model support the idea that g_{min} can have a significant impact on plant survival during drought, which is directly tied to water loss and the prevention of water potentials exceeding lethal thresholds. The SurEau simulations predict an approximate two-week difference before mortality when a positive temperature dependence is assumed for g_{min} compared with a negative dependence with the input parameters from our study. These results, however, need to be considered carefully within the context and assumptions of the SurEau model, particularly given that we had limited access to many of the key traits used to populate the model. It is also important to note that the model, while incorporating hydraulic failure thresholds for mortality, is also largely driven by g_{min} once water potentials drop below the threshold that induces stomatal closure. Yet, the model results highlight the benefits of g_{min} exhibiting a negative temperature dependence for plant survival compared with a positive or neutral temperature dependence, as well as provide some additional motivation for considering g_{min} in landscape model estimates.

Materials and methods

Study sites and species

We selected 24 oak species (genus *Quercus* and subgenus *Quercus*) for this study, 12 from each of two botanical gardens, the California Botanic Garden (CBG) in Claremont, CA, USA (MC), and the Arnold Arboretum in Boston, MA, USA (TC; Table 1; Supplementary Table S1). The selected species spanned four of the *Quercus* sections, *Quercus*, *Lobatae*, *Cerris*, and *Protoblanus*, and three phenologies, evergreen, deciduous, and brevideciduous (Cavender-Bares 2019; Kremer and Hipp 2020; Furze et al. 2021). Using this congeneric sampling framework enabled us to study closely related species with a wide range of anatomical and phenological traits that have a putative link to the temperature response of g_{min}. We collected south facing, sun-exposed branches of ~1 m in length from three individuals per species >10 cm in diameter at breast height in the mornings from May to August of 2022 and May of 2023. Samples were stored in plastic bags with moist paper towels and transported to the laboratory. Branches were recut under water and rehydrated overnight in buckets filled with deionized water and covered with black plastic bags.

Measuring g_{min} temperature and VPD response

To measure g_{min} at different temperatures, we constructed a temperature and humidity controlled chamber with an internal volume of 3,971 cm^3 (19 × 19 × 11 cm) from a fiberglass water- and air-tight box (model PTQ-11055-C, BUD Industries Inc., Willoughby, OH, USA) fitted with two 50-mm cooling fans (WINSINN Inc., China) centrally positioned and at opposing directions to ensure air mixing, a fine-wire thermocouple to monitor air temperature, and bev-a-line tubing attached to a Li-Cor 6800 gas exchange system using the custom–chamber interface (6800-19, LI-COR Inc., Lincoln, NE, USA). The Li-Cor 6800 was used to condition the chamber air to 30% RH and 25 °C (VPD = 2.2 kPa), 35 °C (VPD = 3.9 kPa), or 45 °C (VPD = 6.6 kPa). Prior to all g_{min} measurements, we excised leaves at the petiole–branch junction, sealed the petiole with cyanoacrylite glue (Loctite 409, Henkle Co., Rocky Hill, CT), and dehydrated the leaves for at least an hour suspended above a fan under ambient laboratory conditions following standardized protocols (Sack et al. 2011). To measure g_{min}, we used a gravimetric method, which relies on the curve of change in leaf water mass over time after stomata are assumed to be closed, measured under defined evaporative conditions (Sinclair and Ludlow 1986; Sack et al. 2011). The g_{min} is then calculated from the rate of water loss divided by the driving force, which can be expressed in multiple ways and here as the difference in the mole fraction of water between the leaf and surrounding atmosphere (Schuster et al. 2017). This calculation, standardized by LA has the advantage of allowing for direct comparisons with stomatal conductance measurements using the same units of mmol m^{-2} s^{-1} (Duursma et al. 2019; Slot et al. 2021).

To investigate the temperature response of g_{min}, we conducted 3 experiments (Supplementary Table S2). In the first experiment, we measured g_{min} of two leaves from each individual branch per species and temperature step (25, 35, and 45 °C). At each temperature step, the leaves were suspended by their petioles with adhesive tape in the custom chamber and weighed every 20 min using a high-precision balance (Sartorius Practum224-1S, Sartorius AG, Göttingen, Germany) for ~3 h. Prior to, and at the end of g_{min} measurement, we collected images of the leaves using a digital flatbed scanner to measure initial and final leaf areas. We calculated g_{min} as:

$$g_{min} = \frac{-\Delta mass/\Delta time}{18.0 \times 2 \times LA \times VPD}$$

where $\Delta mass/\Delta time$ is the linear slope of leaf mass over time for the duration of the measurement, 18.0 g mol^{-1} is the molar mass of water, LA is the average of the initial and final leaf areas multiplied by 2 for the two surfaces of the bifacial leaves, and VPD is the mole fraction VPD (mol mol^{-1}). Further, we calculate the linear slope of g_{min} as a function of temperature (Supplementary Table S1). Finally, we calculated the species mean leaf RWC at

the end of the g_{min} measurements to ensure minimal variability in RWC across leaves measured (Supplementary Table S3):

$$RWC = \frac{SWMA - 2 \times LA \times 0.018 \times ([3{,}600 \times g_{min25} \times mfVPD_{lab}] - [3{,}600 \times 3.5 \times g_{min\_treatment} \times mfVPD_{treatment}])}{SWMA \times LA} \times 100$$

where SWMA is the saturated water mass per area (g m^{-2}), LA (m^2) is multiplied by 2 for bifacial leaves, 0.018 g mol^{-1} is the molar mass of water, assuming two phases of leaf dehydration; the first phase on the benchtop under ambient lab conditions for 1 h × 3,600 s h^{-1} and the $mfVPD_{lab}$ is the lab ambient mole fraction VPD (assumed to be 0.016 mol mol^{-1} for a temperature of 25 °C and an RH of 50%) and g_{min} at 25 °C, and the second phase of dehydration inside the custom chamber under different treatment environments for 3.5 h × 3,600 s h^{-1} and the $mfVPD_{treatment}$ is the treatment mole fraction VPD (assumed to be 0.022, 0.039, and 0.066 mol mol^{-1} for temperatures of 25, 35, and 45 °C, respectively, and an RH of 30%), and the $g_{min\_treatment}$ is the species mean g_{min} at each temperature step (Supplementary Table S3).

To test whether the g_{min} temperature responses observed in the first experiment were reversible, we conducted a second experiment using two species with the strongest temperature response (*Q. douglasii* and *Q. durata*) and two species with the weakest temperature response (*Q. rubra* and *Q. coccinea*). This experiment followed a similar protocol to the first experiment described above, with the distinction that g_{min} was measured in the same two leaves per individual at 45 °C for 3 h and then at 25 °C for 2 h. Finally, to cross-validate the measurements from the previous two experiments, we measured g_{min} in one to two leaves from three *Q. rubra* seedlings. Excised leaves sealed with cyanoacrylate glue at the excision site were dehydrated over a box fan for an hour. We then attached the leaves to the Li-Cor 6800 using the standard head attachment (LI-6850) and allowed the leaves to equilibrate at 30% RH and either 25 or 45 °C. At equilibrium, we logged the leaf water conductance every minute for 5 min with the Li-Cor 6800 before the temperature was increased to 45 °C or decreased to 25 °C and logged after equilibrium every minute for another 5 min. The g_{min} of each leaf at each temperature step was then calculated as the 5-min average of leaf water conductance.

Scanning electron microscopy

To determine the surface structure of each species and observe trichome presence or absence, we used environmental scanning electron microscopy (ESEM). Three to five leaves from each individual were collected from rehydrated branches and placed in plastic bags. Leaves from CA, USA, were kept in the fridge and shipped overnight with ice packs and wet paper towels to New Haven, CT, USA, where they were stored in a −80 °C freezer. Leaves collected from MA, USA, were similarly placed in plastic bags and directly stored in a −80 °C freezer after branches were rehydrated overnight. We then removed frozen leaves from the freezer, allowed them to equilibrate at room temperature, and collected leaf discs using a cork borer with a 3-mm inner diameter. Discs were then mounted onto an ESEM sample holder and coated with ~20 nm of carbon. We imaged each sample using ESEM at an accelerating voltage of 10 kV (FEI-XL30, Hillsboro, OR, USA) at 500× magnification and classified each species based on its cuticular surface texture (Gülz 1994). We found that all species either had a cuticle composed of large smooth platelets (classified as smooth; Fig. 1; Table 1; Supplementary Table S1) or a matrix of epicuticular rods (classified as rough; Fig. 1; Table 1; Supplementary Table S1). We then recorded the presence or absence of trichomes on that abaxial and adaxial surfaces.

X-ray computed microtomography

To investigate how stomatal aperture responds to increasing temperature in dark-adapted leaves, we selected the 2 species with the highest g_{min} at 25 °C and the greatest slope for g_{min} between 25 and 45 °C, *Q. douglasii* and *Q. durata*. We chose 2 species that showed the strongest g_{min} temperature response, which would provide us with the highest probability to visually assess whether these strong changes in g_{min} in response to temperature were due to changes in stomatal aperture but were restricted in the total amount of time we had access to the micro-CT instrument and, as a consequence, were unable to work with more than those 2 species. We imaged one to six leaves from each of three individuals per species at 25 or 45 °C using X-ray micro-CT at the Lawrence Berkeley National Laboratory, beamline 8.3.2, in Berkeley, CA, USA. Branches were rehydrated overnight. The following day, leaves were prepared using the same methods for measuring g_{min}, whereas they were excised from the branch, their petioles were sealed with glue and were allowed to dehydrate on the benchtop for 60 to 120 min, and prior to measurement they were wrapped in polyimide tape (Théroux-Rancourt et al. 2017) and then mounted in a custom temperature-controlled chamber equipped with a thermocouple and heating element to control the ambient temperature (Supplementary Fig. S2). The chamber was covered with a polystyrene cup for insulation and to ensure leaves were in a dark environment. The custom chamber was connected to a Li-Cor 6800 with the custom chamber interface using bev-a-line tubing and supplied with air conditioned to 30% RH and 25 or 45 °C into the chamber at a rate of 600 μmol s^{-1}. The custom chamber was mounted to the stage, centered, and then each leaf was scanned at 25 or 45 °C at 10× magnification, yielding a voxel size of 0.27 μm^3. Each scan yielded a stack of 1,092 images, which were reconstructed into a 3D dataset using the *tomopy* software package (Théroux-Rancourt et al. 2017). Images were analyzed in FIJI image analysis software (Schneider et al. 2012). From these scans, we counted the number of open and closed stomata in the field of view (average of 0.18 mm^2 of tissue per leaf) and measured the stomatal pore aperture by observing each stomate in the transverse or paradermal plane (Supplementary Table S5). We measured the stomatal pore area of 33 stomata from each of three individuals per species per temperature step and assigned a stomatal pore area of 0 μm for stomata that appeared to be closed (Supplementary Table S5).

To estimate how total stomatal pore area influences g_{min}, we used the species mean empirically measured stomatal dimensions from micro-CT images (one to six leaves from each of three individuals per species per temperature step) and equations that relate stomatal pore area to leaf gas exchange capacity governed by the physics of diffusion through pores (Franks and Beerling 2009; Dow et al. 2014; Franks et al. 2014; Sack and Buckley 2016; Henry et al. 2019):

$$g_s = \frac{\frac{d}{\upsilon} \times SD \times a \times \%\ \text{open stomata}}{l + 0.5\,\pi\sqrt{\frac{a}{\pi}}} \times 1{,}000$$

where g_s is the anatomical stomatal conductance through partially open stomata (mmol m^{-2} s^{-1}), d is the diffusivity of water through air (2.49×10^{-5} m^2 s^{-1}), υ is the molar volume of air (2.24×10^{-2} m^3 mol^{-1}), SD is the stomatal density (m^{-2}), a is the stomatal pore area (m^2), and l is the guard cell depth (m; assumed to be equal to guard cell width; Franks and Beerling 2009) measured from micro-CT images. To estimate the percent decline in conductance as a result of changes in a between 25 and 45 °C, we calculated g_s

at 25 °C (g_{s25}) and at 45 °C (g_{s45}) and estimated the percent change in conductance as $(g_{s25}-g_{s45})/g_{s25}\times 100$ (Supplementary Table S5).

Leaf trait measurements

We measured the fresh LA (cm^2) in three rehydrated leaves per individual by collecting digital images using a flatbed scanner and measured their area using ImageJ (Supplementary Table S6). We also measured LMA ($g\ m^{-2}$) in three leaves from each individual by collecting fresh LA using a flatbed scanner and drying the leaves at 70 °C for 1 wk prior to measuring dry mass. We measured the fresh LA from digital images using FIJI image analysis software and calculated LMA as the leaf dry mass/leaf fresh LA (Supplementary Table S7). We also measured leaf lamina thickness (LT; mm) in three leaves from each individual, using calipers (IP54 digital Calipers ±0.02 mm, Reeson Inc., Childersburg, AL, USA), averaging three LT measurements per leaf, avoiding any major veins (Supplementary Table S7). We measured SD (mm^{-2}) from stomatal peels from one to three individuals per species (excluding species and individuals that were too hairy to accurately measure SD) in a total of 18 species (Supplementary Table S7). For one to three leaves per individual, we coated the abaxial leaf surface with clear nail polish (Sally Hansen, New York, NY, USA), mounted the dry nail polish peels on microscope slides, and imaged at 200× magnification using a Canon 6D DSLR (Canon, New York, NY, USA) camera mounted to an Olympus BX51 (Olympus Optical, Tokyo, Japan) compound microscope. We counted all the stomata in the field of view using FIJI and calculated SD as # of stomata/area. Finally, we calculated trichome density in one to two leaves from one to three individuals in a subset of five species (*Q. agrifolia*, *Q. berberidifolia*, *Q. douglasii*, *Q. kelloggii*, and *Q. lobata*) collected from the CBG for which we had micro-CT images. Using the micro-CT images of leaves, we counted all trichomes on the abaxial surface as none of the species had trichomes on the adaxial surface and calculated trichome density as the number of trichomes per LA (mm^{-2}; Supplementary Table S7).

Drought simulation using a trait-based plant hydraulics model

To determine the proximate and ultimate effects of g_{min} on tree mortality, we simulated the effects of a two-month long drought on plant water status and drought-induced mortality under three scenarios of g_{min} dependence on air temperature (positive, no relationship, and negative) and two environmental scenarios (MC and TCs) using a trait-based plant hydraulics model, SurEau-Ecos v. 2.0 (Cochard et al. 2021; Ruffault et al. 2022). Temperature, RH, wind speed data extracted from NEON eddy-covariance towers at the San Joaquin Experimental Range (SJER; San Joaquin, CA, USA) and Harvard Forest (HF; Petersham, MA, USA), realistic plant trait (John et al. 2018; Henry et al. 2019; Méndez-Alonzo et al. 2019; Ruffault et al. 2022), soil, and diurnal solar irradiance values were used as input parameters (Supplementary Table S8). We chose environmental variables from each site for 2 mo, which include the highest recorded maximum temperatures from 2022 including some of the highest recorded since 2014 at each site (September 01 2022 to October 31 2022 for SJER and July 15 2022 to September 14 2022 for HF). Simulations were initiated at negligible soil moisture content with no additional precipitation inputs leading to continuous declines in soil and plant water potentials.

The SurEau-Ecos model defines plant mortality based on a set threshold of leaf percent loss of conductivity (PLC), as accurate predictions of moisture content require the additional integration of carbon metabolism (Martinez-Vilalta et al. 2019) not currently implemented in the model (Ruffault et al. 2022). We therefore set the PLC mortality threshold at 99% loss of leaf hydraulic conductivity to guarantee that plant water pools are almost empty and no other water reserves are available for the plant (Ruffault et al. 2022). For all simulations across all species, we used the same soil, diurnal solar irradiance, and plant trait parameters other than those related to g_{min}.

To test the effects of the relationship direction between g_{min} and temperature, we used two systems of two equations relating g_{min} to T_L, either positively or negatively, or maintained g_{min} constant using empirically measured g_{min} values at 25 °C for each species. In the case where g_{min} and T_L are related positively, we used default equations from the SurEau model (Cochard et al. 2021; Ruffault et al. 2022) where the T_L is directly related to air temperature and is computed by solving the leaf's energy budget (Ruffault et al. 2022). Given that g_{min} is assumed to display a biphasic response to temperature above or below a phase transition temperature (T_{phase}, °C), the equation relating g_{min} to T_L follows a single or double Q_{10} (i.e. the g_{min} temperature dependence parameter) equation depending on whether T_L is above or below T_{phase} following equation (1) (Cochard et al. 2021; Ruffault et al. 2022):

if $T_L < T_{phase}$ then,

$$g_{min} = g_{min20}\, Q_{10a}^{\frac{T_L-20}{10}}, \tag{1a}$$

and if $T_L > T_{phase}$ then,

$$g_{min} = g_{min20}\, Q_{10a}^{\frac{T_{phase}-20}{10}}\, Q_{10b}^{\frac{T_L-T_{phase}}{10}}, \tag{1b}$$

where g_{min20} is g_{min} at 20 °C (assumed equal to g_{min} we measured at 25 °C) and Q_{10a} and Q_{10b} are the Q_{10} values of the relationship below and above T_{phase} and assumed to be equal to 1.2 and 4.8, respectively (Cochard 2021; Cochard et al. 2021; Ruffault et al. 2022). We set T_{phase} to be equal to 35 °C to ensure that both systems of equations are analogous in the temperature at which the biphasic slope of $g_{min}(T_L)$ changes.

In the case where g_{min} and T_L are related negatively, we used empirically derived equations from our measured g_{min} responses to air temperature (T_{air}) and assumed that the same empirical relationship applies to g_{min} and T_L. Similar to the SurEau model, we used a biphasic system of equations depending on whether T_L was above or below T_{phase} as the slope of g_{min} as a function of temperature in our measured species differed significantly (*t*-test $P=0.001$; Supplementary Fig. S1) between 25 and 35 °C ($slope_{25\ to\ 35}$) and 35 and 45 °C ($slope_{35\ to\ 45}$). For simplicity and lack of measured data at finer temperature scales, we assumed a linear relationship between each temperature step following equation (2):

if $T_L < T_{phase}$ then,

$$g_{min} = slope_{25\ to\ 35}\ T_L + int_{25\ to\ 35}, \tag{2a}$$

and if $T_L > T_{phase}$ then,

$$g_{min} = slope_{35\ to\ 45}\ T_L + int_{35\ to\ 45}, \tag{2b}$$

where $int_{25\ to\ 35}$ and $int_{35\ to\ 45}$ are the intercepts of the empirical relationship between g_{min} and T_{air} between 25 and 35 °C and 35 and 45 °C, respectively.

Statistical analyses

We conducted 1-way ANOVA using the aov() function in the stats R package to test for differences in g_{min} and its slope as a function of temperature between species with different phenologies, climates, cuticular surface texture, and belonging to different

Quercus sections excluding *Protoblanus* for which we only had one representative species (Table 1). Further, to compare stomatal pore area and the percent of open stomata between species and temperatures, we conducted a 2-way ANOVA with interactions. All ANOVAs were conducted on log-transformed data to improve normality and homoscedasticity. We also used the ks.test() function in the stats R package to conduct a 2-tailed Kolmogorov–Smirnov test to compare the distributions of stomatal pore area of *Q. douglasii* and *Q. durata* at 25 and 45 °C between species within temperature steps and between temperature steps within species. Finally, we conducted Pearson correlation analyses on untransformed and log-transformed data to test for trait–trait relationships across species (Supplementary Table S4). All statistical analyses were conducted using RStudio version 1.3.959.

Acknowledgments

We are grateful to Dula Parkinson and Harold Barnard of beamline 8.3.2 at the Lawrence Berkeley National Laboratory Advanced Light Source and to Andrew McElrone and Melissa Tamarkin for logistical and technical assistance. We are grateful to the staff at the California Botanic Garden and the Arnold Arboretum, especially James Reed and Michael Dosmann for their logistical support. We are also grateful to Lawren Sack for his discussion of the manuscript.

Author contributions

J.Z. and C.R.B. conceived and designed the study. J.Z. collected the data and analyzed the data with guidance and input from C.R.B. and C.S. J.Z. and C.R.B. wrote the first draft, and all authors contributed substantial revisions to the manuscript.

Supplementary data

The following materials are available in the online version of this article.

Supplementary Figure S1. The measured response of g_{min} to increasing ambient temperature in 24 *Quercus* species from the Arnold Arboretum (AA) and the California Botanic Garden (CBG).

Supplementary Figure S2. Schematic sketch of the custom environmental chamber used for micro-CT imaging done in this study.

Supplementary Table S1. Species-level means for measured g_{min} and leaf traits for 24 *Quercus* species.

Supplementary Table S2. Leaf- and individual-level means for g_{min} temperature response data for 24 *Quercus* species.

Supplementary Table S3. Calculation of the species mean RWC of leaves measured for g_{min}.

Supplementary Table S4. Pearson correlation matrix for all traits measured in this study.

Supplementary Table S5. Leaf- and individual-level micro-CT measurement data for two *Quercus* species.

Supplementary Table S6. Diffusion modeling results following Franks and Beerling (2009) equations for two *Quercus* species.

Supplementary Table S7. Leaf- and individual-level trait data measured in this study for 24 *Quercus* species.

Supplementary Table S8. SurEau-Ecos vegetation, climate, and soil input parameters for all simulations.

Funding

This work was funded by the Yale Institute for Biospheric Studies Small Grants program. The Advanced Light Source is supported by the Director, Office of Science, Office of Basic Energy Sciences, of the US Department of Energy under contract no. DE-AC02-05CH11231.

Conflict of interest statement. None declared.

Data availability

All data pertaining to the manuscript are included in the supplementary material.

References

Barbour MM, Cernusak LA, Whitehead D, Griffin KL, Turnbull MH, Tissue DT, Farquhar GD. Nocturnal stomatal conductance and implications for modelling $\delta^{18}O$ of leaf-respired CO_2 in temperate tree species. *Funct Plant Biol*. 2005:32(12):1107. https://doi.org/10.1071/FP05118

Benyon RG. Nighttime water use in an irrigated *Eucalyptus grandis* plantation. *Tree Physiol*. 1999:19(13):853–859. https://doi.org/10.1093/treephys/19.13.853

Bi H, Kovalchuk N, Langridge P, Tricker PJ, Lopato S, Borisjuk N. The impact of drought on wheat leaf cuticle properties. *BMC Plant Biol*. 2017:17(1):85. https://doi.org/10.1186/s12870-017-1033-3

Binstock BR, Manandhar A, McAdam SAM. Characterizing the breakpoint of stomatal response to vapor pressure deficit in an angiosperm. *Plant Physiol*. 2024:194:732–740. https://doi.org/10.1093/plphys/kiad560

Boyer JS. Turgor and the transport of CO_2 and water across the cuticle (epidermis) of leaves. *J Exp Bot*. 2015:66(9):2625–2633. https://doi.org/10.1093/jxb/erv065

Boyer JS, Wong SC, Farquhar GD. CO_2 and water vapor exchange across leaf cuticle (epidermis) at various water potentials. *Plant Physiol*. 1997:114(1):185–191. https://doi.org/10.1104/pp.114.1.185

Brodribb TJ, McAdam SAM, Jordan GJ, Martins SCV. Conifer species adapt to low-rainfall climates by following one of two divergent pathways. *Proc Natl Acad Sci U S A*. 2014:111(40):14489–14493. https://doi.org/10.1073/pnas.1407930111

Brodribb TJ, Powers J, Cochard H, Choat B. Hanging by a thread? Forests and drought. *Science (1979)*. 2020:368:261–266. https://doi.org/10.1126/science.aat7631

Bucci SJ, Goldstein G, Meinzer FC, Franco AC, Campanello P, Scholz FG. Mechanisms contributing to seasonal homeostasis of minimum leaf water potential and predawn disequilibrium between soil and plant water potential in Neotropical savanna trees. *Trees*. 2005:19(3):296–304. https://doi.org/10.1007/s00468-004-0391-2

Bueno A, Alfarhan A, Arand K, Burghardt M, Deininger A-C, Hedrich R, Leide J, Seufert P, Staiger S, Riederer M. Effects of temperature on the cuticular transpiration barrier of two desert plants with water-spender and water-saver strategies. *J Exp Bot*. 2019:70(5):1613–1625. https://doi.org/10.1093/jxb/erz018

Burghardt M, Burghardt A, Gall J, Rosenberger C, Riederer M. Ecophysiological adaptations of water relations of *Teucrium chamaedrys* L. to the hot and dry climate of xeric limestone sites in Franconia (Southern Germany). Flora: Morphology, Distribution. *Funct Ecol Plants*. 2008:203(1):3–13. https://doi.org/10.1016/j.flora.2007.11.003

Burghardt M, Riederer M. Ecophysiological relevance of cuticular transpiration of deciduous and evergreen plants in relation to stomatal closure and leaf water potential. *J Exp Bot*. 2003:54(389):1941–1949. https://doi.org/10.1093/jxb/erg195

Caird MA, Richards JH, Donovan LA. Nighttime stomatal conductance and transpiration in C_3 and C_4 plants. *Plant Physiol.* 2007:143(1):4–10. https://doi.org/10.1104/pp.106.092940

Cameron KD, Teece MA, Smart LB. Increased accumulation of cuticular wax and expression of lipid transfer protein in response to periodic drying events in leaves of tree tobacco. *Plant Physiol.* 2006:140(1):176–183. https://doi.org/10.1104/pp.105.069724

Cardoso AA, Brodribb TJ, Kane CN, DaMatta FM, McAdam SAM. Osmotic adjustment and hormonal regulation of stomatal responses to vapour pressure deficit in sunflower. *AoB Plants.* 2020:12(4):plaa025. https://doi.org/10.1093/aobpla/plaa025

Cavender-Bares J. Diversification, adaptation, and community assembly of the American oaks (*Quercus*), a model clade for integrating ecology and evolution. *New Phytol.* 2019:221(2):669–692. https://doi.org/10.1111/nph.15450

Choat B, Brodribb TJ, Brodersen CR, Duursma RA, López R, Medlyn BE. Triggers of tree mortality under drought. *Nature.* 2018:558(7711):531–539. https://doi.org/10.1038/s41586-018-0240-x

Cochard H. A new mechanism for tree mortality due to drought and heatwaves. *Peer Community J.* 2021:1:e36. https://doi.org/10.24072/pcjournal.45

Cochard H, Pimont F, Ruffault J, Martin-StPaul N. SurEau: a mechanistic model of plant water relations under extreme drought. *Ann For Sci.* 2021:78(2):55. https://doi.org/10.1007/s13595-021-01067-y

Daley MJ, Phillips NG. Interspecific variation in nighttime transpiration and stomatal conductance in a mixed New England deciduous forest. *Tree Physiol.* 2006:26(4):411–419. https://doi.org/10.1093/treephys/26.4.411

Dariva FD, Copati MGF, Pessoa HP, Alves FM, de Dias FO, de Picoli EAT, da Cunha FF, Nick C. Evaluation of anatomical and physiological traits of *Solanum pennellii* Cor. associated with plant yield in tomato plants under water-limited conditions. *Sci Rep.* 2020:10(1):16052. https://doi.org/10.1038/s41598-020-73004-4

Dawson TE, Burgess SSO, Tu KP, Oliveira RS, Santiago LS, Fisher JB, Simonin KA, Ambrose AR. Nighttime transpiration in woody plants from contrasting ecosystems. *Tree Physiol.* 2007:27(4):561–575. https://doi.org/10.1093/treephys/27.4.561

Dillen SY, de Beeck MO, Hufkens K, Buonanduci M, Phillips NG. Seasonal patterns of foliar reflectance in relation to photosynthetic capacity and color index in two co-occurring tree species, *Quercus rubra* and *Betula papyrifera*. *Agric For Meteorol.* 2012:160:60–68. https://doi.org/10.1016/j.agrformet.2012.03.001

Dow GJ, Bergmann DC, Berry JA. An integrated model of stomatal development and leaf physiology. *New Phytol.* 2014:201(4):1218–1226. https://doi.org/10.1111/nph.12608

Duursma RA, Blackman CJ, Lopéz R, Martin-StPaul NK, Cochard H, Medlyn BE. On the minimum leaf conductance: its role in models of plant water use, and ecological and environmental controls. *New Phytol.* 2019:221(2):693–705. https://doi.org/10.1111/nph.15395

Eglinton G, Hamilton RJ. Leaf epicuticular waxes. *Science.* 1967:156:1322–1335. https://doi.org/10.1126/science.156.3780.1322

Ehrler WL. Periodic nocturnal stomatal opening of citrus in a steady environment. *Physiol Plant.* 1971:25(3):488–492. https://doi.org/10.1111/j.1399-3054.1971.tb01478.x

Franks PJ, Beerling DJ. Maximum leaf conductance driven by CO_2 effects on stomatal size and density over geologic time. *Proc Natl Acad Sci.* 2009:106(25):10343–10347. https://doi.org/10.1073/pnas.0904209106

Franks PJ, Royer DL, Beerling DJ, Van de Water PK, Cantrill DJ, Barbour MM, Berry JA. New constraints on atmospheric CO_2 concentration for the Phanerozoic. *Geophys Res Lett.* 2014:41(13):4685–4694. https://doi.org/10.1002/2014GL060457

Furze ME, Wainwright DK, Huggett BA, Knipfer T, McElrone AJ, Brodersen CR. Ecologically driven selection of nonstructural carbohydrate storage in oak trees. *New Phytol.* 2021:232(2):567–578. https://doi.org/10.1111/nph.17605

Grossiord C, Buckley TN, Cernusak LA, Novick KA, Poulter B, Siegwolf RTW, Sperry JS, McDowell NG. Plant responses to rising vapor pressure deficit. *New Phytol.* 2020:226(6):1550–1566. https://doi.org/10.1111/nph.16485

Grünhofer P, Herzig L, Schreiber L. Leaf morphology, wax composition, and residual (cuticular) transpiration of four poplar clones. *Trees.* 2022:36(2):645–658. https://doi.org/10.1007/s00468-021-02236-2

Gülz P-G. Epicuticular leaf waxes in the evolution of the plant kingdom. *J Plant Physiol.* 1994:143(4–5):453–464. https://doi.org/10.1016/S0176-1617(11)81807-9

Hamerlynck E, Knapp AK. Photosynthetic and stomatal responses to high temperature and light in two oaks at the western limit of their range. *Tree Physiol.* 1996:16(6):557–565. https://doi.org/10.1093/treephys/16.6.557

Hammond WM, Adams HD. Dying on time: traits influencing the dynamics of tree mortality risk from drought. *Tree Physiol.* 2019:39(6):906–909. https://doi.org/10.1093/treephys/tpz050

Hammond WM, Williams AP, Abatzoglou JT, Adams HD, Klein T, López R, Sáenz-Romero C, Hartmann H, Breshears DD, Allen CD. Global field observations of tree die-off reveal hotter-drought fingerprint for Earth's forests. *Nat Commun.* 2022:13(1):1761. https://doi.org/10.1038/s41467-022-29289-2

Hartill GE, Blackman CJ, Halliwell B, Jones RC, Holland BR, Brodribb TJ. Cold temperature and aridity shape the evolution of drought tolerance traits in Tasmanian species of *Eucalyptus*. *Tree Physiol.* 2023:43(9):1493–1500. https://doi.org/10.1093/treephys/tpad065

Henry C, John GP, Pan R, Bartlett MK, Fletcher LR, Scoffoni C, Sack L. A stomatal safety-efficiency trade-off constrains responses to leaf dehydration. *Nat Commun.* 2019:10(1):3398. https://doi.org/10.1038/s41467-019-11006-1

Herrera JC, Calderan A, Gambetta GA, Peterlunger E, Forneck A, Sivilotti P, Cochard H, Hochberg U. Stomatal responses in grapevine become increasingly more tolerant to low water potentials throughout the growing season. *Plant J.* 2022:109(4):804–815. https://doi.org/10.1111/tpj.15591

Hipp AL, Manos PS, Hahn M, Avishai M, Bodénès C, Cavender-Bares J, Crowl AA, Deng M, Denk T, Fitz-Gibbon S, *et al.* Genomic landscape of the global oak phylogeny. *New Phytol.* 2020:226(4):1198–1212. https://doi.org/10.1111/nph.16162

Hlwatika CNM, Bhat RB. An ecological interpretation of the difference in leaf anatomy and its plasticity in contrasting tree species in Orange Kloof, Table Mountain, South Africa. *Ann Bot.* 2002:89(1):109–114. https://doi.org/10.1093/aob/mcf011

Huggins TD, Mohammed S, Sengodon P, Ibrahim AMH, Tilley M, Hays DB. Changes in leaf epicuticular wax load and its effect on leaf temperature and physiological traits in wheat cultivars (*Triticum aestivum* L.) exposed to high temperatures during anthesis. *J Agron Crop Sci.* 2018:204(1):49–61. https://doi.org/10.1111/jac.12227

John GP, Henry C, Sack L. Leaf rehydration capacity: associations with other indices of drought tolerance and environment. *Plant Cell Environ.* 2018:41(11):2638–2653. https://doi.org/10.1111/pce.13390

Jordan GJ, Brodribb TJ. Incontinence in aging leaves: deteriorating water relations with leaf age in *Agastachys odorata* (Proteaceae),

a shrub with very long-lived leaves. *Funct Plant Biol*. 2007:34(10): 918–924. https://doi.org/10.1071/FP07166

Jurik TW. Seasonal patterns of leaf photosynthetic capacity in successional northern hardwood tree species. *Am J Bot*. 1986:73(1): 131–138. https://doi.org/10.1002/j.1537-2197.1986.tb09688.x

Kane CN, Jordan GJ, Jansen S, McAdam SAM. A permeable cuticle, not open stomata, is the primary source of water loss from expanding leaves. *Front Plant Sci*. 2020:11:774. https://doi.org/10.3389/fpls.2020.00774

Kerstiens G. Cuticular water permeability and its physiological significance. *J Exp Bot*. 1996:47(12):1813–1832. https://doi.org/10.1093/jxb/47.12.1813

Koch K, Barthlott W. Plant epicuticular waxes: chemistry, form, self-assembly and function. *Nat Prod Commun*. 2006:1: 1934578X0600101 123. https://doi.org/10.1177/1934578X0600101123

Koch K, Ensikat H-J. The hydrophobic coatings of plant surfaces: epicuticular wax crystals and their morphologies, crystallinity and molecular self-assembly. *Micron*. 2008:39(7):759–772. https://doi.org/10.1016/j.micron.2007.11.010

Kremer A, Hipp AL. Oaks: an evolutionary success story. *New Phytol*. 2020:226(4):987–1011. https://doi.org/10.1111/nph.16274

Liang X, Wang D, Ye Q, Zhang J, Liu M, Liu H, Yu K, Wang Y, Hou E, Zhong B, *et al*. Stomatal responses of terrestrial plants to global change. *Nat Commun*. 2023:14(1):2188. https://doi.org/10.1038/s41467-023-37934-7

Loewenstein NJ, Pallardy SG. Drought tolerance, xylem sap abscisic acid and stomatal conductance during soil drying: a comparison of canopy trees of three temperate deciduous angiosperms. *Tree Physiol*. 1998:18(7):431–439. https://doi.org/10.1093/treephys/18.7.431

Lombardozzi DL, Zeppel MJB, Fisher RA, Tawfik A. Observed nighttime conductance alters modeled global hydrology and carbon budgets. *Geosci Model Dev Discuss*. 2015:8:10339–10363. https://doi.org/10.5194/gmdd-8-10339-2015

Machado R, Loram-Lourenço L, Farnese FS, Alves RDFB, Sousa LF, Silva FG, Filho SCV, Torres-Ruiz JM, Cochard H, Menezes-Silva PE. Where do leaf water leaks come from? Trade-offs underlying the variability in minimum conductance across tropical savanna species with contrasting growth strategies. *New Phytol*. 2021:229(3):1415–1430. https://doi.org/10.1111/nph.16941

Mansfield TA. Studies in stomatal behaviour: XII. Opening in high temperature in darkness. *J Exp Bot*. 1965:16(4):721–731. https://doi.org/10.1093/jxb/16.4.721

Marchin RM, Backes D, Ossola A, Leishman MR, Tjoelker MG, Ellsworth DS. Extreme heat increases stomatal conductance and drought-induced mortality risk in vulnerable plant species. *Glob Chang Biol*. 2022:28(3):1133–1146. https://doi.org/10.1111/gcb.15976

Marks CO, Lechowicz MJ. The ecological and functional correlates of nocturnal transpiration. *Tree Physiol*. 2007:27(4):577–584. https://doi.org/10.1093/treephys/27.4.577

Márquez DA, Stuart-Williams H, Farquhar GD. An improved theory for calculating leaf gas exchange more precisely accounting for small fluxes. *Nat Plants*. 2021:7(3):317–326. https://doi.org/10.1038/s41477-021-00861-w

Márquez DA, Stuart-Williams H, Farquhar GD, Busch FA. Cuticular conductance of adaxial and abaxial leaf surfaces and its relation to minimum leaf surface conductance. *New Phytol*. 2022:233(1): 156–168. https://doi.org/10.1111/nph.17588

Martinez-Vilalta J, Anderegg WRL, Sapes G, Sala A. Greater focus on water pools may improve our ability to understand and anticipate drought-induced mortality in plants. *New Phytol*. 2019:223(1):22–32. https://doi.org/10.1111/nph.15644

Martin-StPaul N, Delzon S, Cochard H. Plant resistance to drought depends on timely stomatal closure. *Ecol Lett*. 2017:20(11):1437–1447. https://doi.org/10.1111/ele.12851

Mathur S, Agrawal D, Jajoo A. Photosynthesis: response to high temperature stress. *J Photochem Photobiol B*. 2014:137:116–126. https://doi.org/10.1016/j.jphotobiol.2014.01.010

Matsumoto Y, Tanaka T, Kosuge S, Tanbara T, Uemura A, Shigenaga H, Ishida A, Okuda S, Maruyama Y, Morikawa Y. Maximum gas exchange rates in current sun leaves of 41 deciduous and evergreen broad-leaved tree species in Japan. *J Forest Environ*. 1999:41:113–121. https://doi.org/10.18922/jjfe.41.2_113

McDowell NG, Sapes G, Pivovaroff A, Adams HD, Allen CD, Anderegg WRL, Arend M, Breshears DD, Brodribb T, Choat B, *et al*. Mechanisms of woody-plant mortality under rising drought, CO_2 and vapour pressure deficit. *Nat Rev Earth Environ*. 2022:3(5): 294–308. https://doi.org/10.1038/s43017-022-00272-1

Meinzer FC, Smith DD, Woodruff DR, Marias DE, McCulloh KA, Howard AR, Magedman AL. Stomatal kinetics and photosynthetic gas exchange along a continuum of isohydric to anisohydric regulation of plant water status. *Plant Cell Environ*. 2017:40(8): 1618–1628. https://doi.org/10.1111/pce.12970

Méndez-Alonzo R, Ewers FW, Jacobsen AL, Pratt RB, Scoffoni C, Bartlett MK, Sack L. Covariation between leaf hydraulics and biomechanics is driven by leaf density in Mediterranean shrubs. *Trees*. 2019:33(2):507–519. https://doi.org/10.1007/s00468-018-1796-7

Merilo E, Yarmolinsky D, Jalakas P, Parik H, Tulva I, Rasulov B, Kilk K, Kollist H. Stomatal VPD response: there is more to the story than ABA. *Plant Physiol*. 2018:176(1):851–864. https://doi.org/10.1104/pp.17.00912

Mills C, Bartlett MK, Buckley TN. The poorly-explored stomatal response to temperature at constant evaporative demand. *Plant Cell Environ*. 2024:47(9):3428–3446. https://doi.org/10.1111/pce.14911

Mott KA, Peak D. Stomatal responses to humidity and temperature in darkness. *Plant Cell Environ*. 2010:33(7):1084–1090. https://doi.org/10.1111/j.1365-3040.2010.02129.x

Muchow RC, Sinclair TR. Epidermal conductance, stomatal density and stomatal size among genotypes of *Sorghum bicolor* (L.) Moench. *Plant Cell Environ*. 1989:12(4):425–431. https://doi.org/10.1111/j.1365-3040.1989.tb01958.x

Musselman RC, Minnick TJ. Nocturnal stomatal conductance and ambient air quality standards for ozone. *Atmos Environ*. 2000:34(5): 719–733. https://doi.org/10.1016/S1352-2310(99)00355-6

Nolan RH, Blackman CJ, de Dios VR, Choat B, Medlyn BE, Li X, Bradstock RA, Boer MM. Linking forest flammability and plant vulnerability to drought. *Forests*. 2020:11(7):779. https://doi.org/10.3390/f11070779

Novick KA, Oren R, Stoy PC, Siqueira MBS, Katul GG. Nocturnal evapotranspiration in eddy-covariance records from three co-located ecosystems in the Southeastern U.S.: implications for annual fluxes. *Agric For Meteorol*. 2009:149(9):1491–1504. https://doi.org/10.1016/j.agrformet.2009.04.005

Ochoa ME, Henry C, John GP, Medeiros CD, Pan R, Scoffoni C, Buckley TN, Sack L. Pinpointing the causal influences of stomatal anatomy and behavior on minimum, operational, and maximum leaf surface conductance. *Plant Physiol*. 2024:196(1):51–66. https://doi.org/10.1093/plphys/kiae292

Pemdasa MA. Stomatal responses to high temperature in darkness. *Ann Bot*. 1977:41(5):969–976. https://doi.org/10.1093/oxfordjournals.aob.a085394

Peters JMR, López R, Nolf M, Hutley LB, Wardlaw T, Cernusak LA, Choat B. Living on the edge: a continental-scale assessment of forest vulnerability to drought. *Glob Chang Biol*. 2021:27(15):3620–3641. https://doi.org/10.1111/gcb.15641

POWO. *Plants of the World Online, facilitated by the Royal Botanic Gardens, Kew*. Published on the Internet. 2024. http://www.plantsoftheworldonline.org/

Reich PB, Hinckley TM. Influence of pre-dawn water potential and soil-to-leaf hydraulic conductance on maximum daily leaf diffusive conductance in two oak species. *Funct Ecol*. 1989:3(6):719. https://doi.org/10.2307/2389504

Riederer M, Muller C. Biology of the plant cuticle. *Anal Biochem*. 2006:144:181. https://doi.org/10.1002/9780470988718

Ruffault J, Limousin J, Pimont F, Dupuy J, De Càceres M, Cochard H, Mouillot F, Blackman CJ, Torres-Ruiz JM, Parsons RA, *et al*. Plant hydraulic modelling of leaf and canopy fuel moisture content reveals increasing vulnerability of a Mediterranean forest to wildfires under extreme drought. *New Phytol*. 2023:237(4):1256–1269. https://doi.org/10.1111/nph.18614

Ruffault J, Pimont F, Cochard H, Dupuy J-L, Martin-StPaul N. SurEau-Ecos v2.0: a trait-based plant hydraulics model for simulations of plant water status and drought-induced mortality at the ecosystem level. *Geosci Model Dev*. 2022:15(14):5593–5626. https://doi.org/10.5194/gmd-15-5593-2022

Sack L, Buckley TN. The developmental basis of stomatal density and flux. *Plant Physiol*. 2016:171(4):2358–2363. https://doi.org/10.1104/pp.16.00476

Sack L, Scoffoni C, PrometheusWiki contributors. Protocol: minimum epidermal conductance (g_{min}, a.k.a. cuticular conductance). PrometheusWiki. 2011 https://prometheusprotocols.net/function/gas-exchange-and-chlorophyll-fluorescence/stomatal-and-non-stomatal-conductance-and-transpiration/minimum-epidermalconductance-gmin-a-k-a-cuticular-conductance/.

Saito K, Futakuchi K. Genotypic variation in epidermal conductance and its associated traits among *Oryza sativa* and *O. glaberrima* cultivars and their interspecific progenies. *Crop Sci*. 2010:50(1):227–234. https://doi.org/10.2135/cropsci2009.06.0284

Šantrůček J, Šimáňová E, Karbulková J, Šimková M, Schreiber L. A new technique for measurement of water permeability of stomatous cuticular membranes isolated from *Hedera helix* leaves. *J Exp Bot*. 2004:55(401):1411–1422. https://doi.org/10.1093/jxb/erh150

Saruwatari MW, Davis SD. Tissue water relations of three chaparral shrub species after wildfire. *Oecologia*. 1989:80(3):303–308. https://doi.org/10.1007/BF00379031

Schäfer KVR. Canopy stomatal conductance following drought, disturbance, and death in an upland oak/pine forest of the New Jersey Pine Barrens, USA. *Front Plant Sci*. 2011:2:1–7. https://doi.org/10.3389/fpls.2011.00015

Schneider CA, Rasband WS, Eliceiri KW. NIH image to ImageJ: 25 years of image analysis. *Nat Methods*. 2012:9(7):671–675. https://doi.org/10.1038/nmeth.2089

Schreiber L. Effect of temperature on cuticular transpiration of isolated cuticular membranes and leaf discs. *J Exp Bot*. 2001:52(362):1893–1900. https://doi.org/10.1093/jexbot/52.362.1893

Schuster AC, Burghardt M, Alfarhan A, Bueno A, Hedrich R, Leide J, Thomas J, Riederer M. Effectiveness of cuticular transpiration barriers in a desert plant at controlling water loss at high temperatures. *AoB Plants*. 2016:8:plw027. https://doi.org/10.1093/aobpla/plw027

Schuster A-C, Burghardt M, Riederer M. The ecophysiology of leaf cuticular transpiration: are cuticular water permeabilities adapted to ecological conditions? *J Exp Bot*. 2017:68(19):5271–5279. https://doi.org/10.1093/jxb/erx321

Scoffoni C, Kunkle J, Pasquet-Kok J, Vuong C, Patel AJ, Montgomery RA, Givnish TJ, Sack L. Light-induced plasticity in leaf hydraulics, venation, anatomy, and gas exchange in ecologically diverse Hawaiian lobeliads. *New Phytol*. 2015:207(1):43–58. https://doi.org/10.1111/nph.13346

Seufert P, Staiger S, Arand K, Bueno A, Burghardt M, Riederer M. Building a barrier: the influence of different wax fractions on the water transpiration barrier of leaf cuticles. *Front Plant Sci*. 2022:12:766602. https://doi.org/10.3389/fpls.2021.766602

Sharma P, Kothari SL, Rathore MS, Gour VS. Properties, variations, roles, and potential applications of epicuticular wax: a review. *Turk J Botany*. 2018:42(2):135–149. https://doi.org/10.3906/bot-1702-25

Sinclair T, Ludlow M. Influence of soil water supply on the plant water balance of four tropical grain legumes. *Funct Plant Biol*. 1986:13(3):329. https://doi.org/10.1071/PP9860329

Slot M, Nardwattanawong T, Hernández GG, Bueno A, Riederer M, Winter K. Large differences in leaf cuticle conductance and its temperature response among 24 tropical tree species from across a rainfall gradient. *New Phytol*. 2021:232(4):1618–1631. https://doi.org/10.1111/nph.17626

Smith SE, Fendenheim DM, Halbrook K. Epidermal conductance as a component of dehydration avoidance in *Digitaria californica* and *Eragrostis lehmanniana*, two perennial desert grasses. *J Arid Environ*. 2006:64(2):238–250. https://doi.org/10.1016/j.jaridenv.2005.04.012

Théroux-Rancourt G, Earles JM, Gilbert ME, Zwieniecki MA, Boyce CK, McElrone AJ, Brodersen CR. The bias of a two-dimensional view: comparing two-dimensional and three-dimensional mesophyll surface area estimates using noninvasive imaging. *New Phytol*. 2017:215(4):1609–1622. https://doi.org/10.1111/nph.14687

Wang C, He J, Zhao T-H, Cao Y, Wang G, Sun B, Yan X, Guo W, Li M-H. The smaller the leaf is, the faster the leaf water loses in a temperate forest. *Front Plant Sci*. 2019:10:1–12. https://doi.org/10.3389/fpls.2019.00001

Wang S, Hoch G, Grun G, Kahmen A. Water loss after stomatal closure: quantifying leaf minimum conductance and minimal water use in 9 temperate *European* tree species during a severe drought. *Tree Physiol*. 2024:44(4):tpae027. https://doi.org/10.1093/treephys/tpae027

Wilson KB, Baldocchi DD, Hanson PJ. Quantifying stomatal and non-stomatal limitations to carbon assimilation resulting from leaf aging and drought in mature deciduous tree species. *Tree Physiol*. 2000:20(12):787–797. https://doi.org/10.1093/treephys/20.12.787

Xu L, Baldocchi DD. Seasonal trends in photosynthetic parameters and stomatal conductance of blue oak (*Quercus douglasii*) under prolonged summer drought and high temperature. *Tree Physiol*. 2003:23(13):865–877. https://doi.org/10.1093/treephys/23.13.865

Yeats TH, Rose JKC. The formation and function of plant cuticles. *Plant Physiol*. 2013:163(1):5–20. https://doi.org/10.1104/pp.113.222737

Yuan W, Zheng Y, Piao S, Ciais P, Lombardozzi D, Wang Y, Ryu Y, Chen G, Dong W, Hu Z, *et al*. Increased atmospheric vapor pressure deficit reduces global vegetation growth. *Sci Adv*. 2019:5(8):1–12. https://doi.org/10.1126/sciadv.aax1396

Zhang Q, Shao M, Jia X, Wei X. Relationship of climatic and forest factors to drought- and heat-induced tree mortality. *PLoS One*. 2017:12(1):e0169770. https://doi.org/10.1371/journal.pone.0169770

Zhang Y, Du Z, Han Y, Chen X, Kong X, Sun W, Chen C, Chen M. Plasticity of the cuticular transpiration barrier in response to water shortage and resupply in *Camellia sinensis*: a role of cuticular waxes. *Front Plant Sci*. 2021:11:1–17. https://doi.org/10.3389/fpls.2020.600069